Desalination and Water Treatment
www.deswater.com

doi: 10.5004/dwt.2022.28499

262 (2022) 14–26
June

Characteristics of heat transfer and pressure drop in a corrugated plate heat exchanger with chemically synthesized ZnO/sparkling water nanofluids

Anish Mariadhas*, Ignatius Raja, Rahul Kavvampally, Jayaprabakar Jayaraman, Nivin Joy

School of Mechanical Engineering, Sathyabama Institute of Science and Technology,Jeppiar Nagar, Chennai, India, emails: anish2010me@gmail.com (A. Mariadhas), ignatiusraja2@gmail.com (I. Raja), kavvampallyrahul@gmail.com (R. Kavvampally), jp21tn@gmail.com (J. Jayaraman), nivinjoy@gmail.com (N. Joy)

Received 10 December 2021; Accepted 12 April 2022

ABSTRACT

The purpose of this experiment is to investigate the effects of a chemical-based nanofluid consisting of zinc oxides and sparkling water on a heat transfer system. Nanofluids are typically created using ZnO nanoparticles with diameters ranging from 100 nm to 99% purity that have been chemically synthesized in a laboratory. In a corrugated plate heat exchanger, the effects of a chemical-based zinc oxides sparkling/water nanofluid on heat transfer and pressure drop in a heat exchanger employing a domestic hot water system are explored. Their heat transmission qualities are investigated in order to establish their ideal size and weight. The heat transfer coefficient of chemically generated zinc oxide is investigated in terms of weight concentration, Reynolds number, and the presence of nanoparticles. The impact of changing the Reynolds number and weight concentration of chemically produced zinc oxide nanoparticles on their heat transmission properties is investigated. This research demonstrates that increasing the weight of nanoparticles in a heat exchanger may enhance the heat transfer properties of nanofluids. The maximum augmentation of nanofluid's convective heat transfer efficiency is 28.9% for 0.1%, 0.5%, and 1.3% weight fraction of nanoparticles, respectively. This advantage is shown by a decrease in system pressure drop. Therefore, the observed increase in the coefficient of heat transfer is proportional to the volume of nanoparticles present in the system and the pressure decrease experienced inside it.

Keywords: Corrugated plate heat exchanger; Zinc oxide; Convective heat transfer coefficient; Pressure drop; Nanofluid

1. Introduction

Heat exchangers are used in more than just refrigerators and air conditioners; heat pumps also employ them. Because of its small diameters and low pressures, the plate heat exchanger is a good choice for efficiency and cost-effectiveness. The creation of a nanoparticle-sized fluid with exceptional dispersion stability has the potential to tackle a wide range of issues, including sedimentation in heat exchanger tubes, pressure drop, and wear on pumps and moving components. According to recent research, meeting needs of the industry requires both the downsizing of massive heat transfer equipment and the use of maximum heat transfer fluids. Miniaturizing the equipment that aids heat transfer inside the industry is no longer a realistic choice as of currently. One of the concepts driving the development of nanofluids for enhanced heat transfer performance is the use of nanofluids to increase heat transfer coefficients while simultaneously lowering the size of large heat transfer equipment. As a result, this application necessitates the use of high-performance, high-temperature fluids with improved flow and heat transmission capabilities. The

* Corresponding author.

working fluids of these fluids can be altered by introducing suspended particulate matter (water, ethylene glycol, oil etc.). Modifying the thermophysical characteristics of the working fluid produces high-performance heat transfer fluids (thermal conductivity, specific heat, density, and viscosity), as well as inserting metallic and non-metallic particles. Several experimental investigations have been conducted in the literature to improve heat transfer efficiency by adding nanofluids into channels with a range of flow shapes. Heris et al. [1] studied metal oxide nanoparticles made up of CuO and Al_2O_3 oxide nanoparticles dissolved in water, as well as laminar flow convective heat transfer around a circular tube with constant wall temperatures. Anoop et al. [2] they observed that Al_2O_3-water nanofluids were successful in increasing the flow area of a tube with continuous heat flux by investigating the heat transfer properties in the improved region of the flow of tube with continuous heat flux. During this experiment, the average particle size was 45 nm, while the particle size utilized in this investigation was 150 nm. In this experiment, it was discovered that the heat transfer capabilities of both nanofluids were much greater than those of the base fluid, with the heat transfer coefficient of the nanofluid with 45 nm particles being significantly higher than that of the nanofluid with 150 nm particles.

Furthermore, the heat transfer coefficient of the nanofluid with 45 nm particles is larger than the heat transfer coefficient of the nanofluid with 150 nm particles in both cases. A 25% improvement in the heat transfer coefficient of nanofluids based on 45 nm particles (4 wt.%) was seen; an 11% improvement was observed for nanofluids based on 150 nm particles. Ahmad et al. [3] reports the numerical investigation of heat transfer and friction factor in nanofluids with laminar flow characteristics in a rectangular channel was carried out. Nanoparticles of Al_2O_3, Cu, and SiO_2 were tested for their capacity to boost heat transfer rates by varying their volume fractions between 0.5% and 2.5%, while maintaining a constant nanoparticle diameter of 25 nm throughout the experiment. Xu and Xu [4] studied flow of boiling heat transfer rate in a single channel using nanofluid (weight concentration of 0.2%, 40 nm) and pure water as working fluids, and their findings were reported in Nature Communications. When compared to regular water, the testing results show that nanofluid improves heat transmission. The heat transfer coefficient of nanofluid is predicted to be around 17% more than that of pure water. Edalati et al. [5] used a CuO/water nanofluid in a laminar flow to evaluate the heat transfer of an equilateral triangular duct in a laminar flow with constant heat flux. The experimental heat transfer coefficient of the CuO/water nanofluid is larger than the heat transfer coefficient of pure water. The experimental heat transfer coefficient of the CuO/water nanofluid is also higher than predicted, indicating a beneficial outcome. At a concentration of 0.8%, CuO/water nanofluid has a convective heat transfer coefficient ratio of 1.41, suggesting that it is extremely heat transfer efficient. Hojjat et al. [6] used three non-Newtonian nanofluids (Al_2O_3, TiO_2, and CuO) in a circular tube with a constant wall temperature. Their results show that nanoparticles increase the convective heat transfer of nano dispersions when compared to the base fluid. The usual increases in Nusselt number for Al_2O_3, CuO and TiO_2 nanofluids with 0.1, 0.25, 0.5, 1.0, and 1.5 volume % of nanoparticles are around 7%, 10%, 12%, 16%, and 19%, respectively. According to Yang et al. [7] the coefficient of heat transfer between graphite-water nanofluids is determined in this study utilizing the nanofluids convective thermal conductivity. Nanofluids with enhanced volume% and Reynolds number may be employed to improve heat exchanger efficiency. The researchers observed that employing nanofluids increased heat transmission by around 19% when compared to using normal water in their experiments. They determined that nanofluids had a higher convective thermal efficiency than ordinary fluids, which they compared to other fluids. Duangthongsuk and Wongwises [8] examined the properties of heat and flow for TiO_2-water nanoparticles in a twin-tube hot air heat exchanger using TiO_2-water nanoparticles. An investigative study by Pantzali et al. [9] evaluated the transfer of heat of TiO_2-water nanofluid and -water in the heat exchanger as part of a larger investigational study. They conducted their research using the aforementioned nanofluids, which included nanoparticle concentrations of 0.3, 0.5, 0.75, 1, and 2% by volume, respectively. The researchers observed that, when compared to distilled water, water and TiO_2-water nanofluids increased convective heat transfer by 19%–56% and 18%–56%, respectively, over distilled water. The performance of multi-channel heat exchangers employing Al_2O_3 water nanofluid was investigated using nanoparticle concentrations of 1% and 0.5% by weight of the fluid, respectively. According to Jwo et al. [10] the influence of these variables on the heat transfer coefficient was also investigated. The heat transmission performance of an Al_2O_3 nanofluid was enhanced by raising its weight concentration to 1% or less of the total weight of the fluid. Chandrasekar et al. [11] investigated the heat transfer of Al_2O_3 water nanofluids via a circular pipe with a wire coil at a nanoparticle concentration of less than 0.01%, which was lower than the industry standard. The use of an aluminium oxide nanofluid with a concentration of 1%–3% weight concentration improves the thermal performance of a heat pipe. According to Moraveji and Razvarz [12] the impact of altering the nanofluid's weight concentration and charging it on the thermal performance of a heat pipe has been investigated. According to Tiwari et al. [13] the heat transfer coefficient of nanofluids rises with volume. This odd occurrence occurs as the nanofluids heat up. The heat transfer coefficient of nanofluids decreases as water volume and nanofluids increase. According to the researchers, the heat transfer efficiency of nanofluids rises by roughly 39% as their temperature decreases. Using a heat exchanger with a chevron pattern. Huang et al. [14] examined the temperature and pressure drop properties of Al_2O_3/water nanofluids and multi-walled carbon nanotubes (MWCNT)/water nanocarriers. In a U-tube heat exchanger, Prasad et al. [15] studied the friction and heat transfer characteristics of Al_2O_3 nanofluids. The Nusselt number may grow as the volume proportion of nanoparticles increases. The temperature distribution and pressure drop properties of Al_2O_3/water nanofluids and MWCNT/water nanocarriers travelling through a chevron-type heat exchanger and these are compared using this method

Ray et al. [16] investigated the heat transfer coefficient and other parameters of nanofluids in a compact plate heat exchanger, and their findings were published in Nature Communications. They discovered that the forced convection heat coefficient increased with each kind of nanofluid used in the experiment. An intricate TiO_2 nanoparticle suspension is disseminated in a combination of ethylene glycol and water and then passed through a heat exchanger. In their research, Reddy and Rao [17] looked into the effects of volume and Reynolds number on the heat transfer coefficient. Wang and Peng [18] investigated liquid forced-convection heat transfer through micro channels and found that for the range of water flow velocities and other experimental conditions used, the Reynolds number for the experiments using micro channeled structures was usually about 500–1,000 at the inlet and about 180 and 2,500 or larger at the outlet. For an intake Reynolds number of only around 1,000, this indicates that the Reynolds number for water flow might be doubled across the length of the micro channel. From the conclusion of literature, this study investigates the effect of zinc oxide nanoparticles, which are created chemically, on the heat transfer characteristics of hot water. This experiment is being carried out in order to determine the efficiency with which zinc oxide nanoparticles disperse in sparkling water after being chemically synthesized. For suspended nanoparticles, the Reynolds numbers are utilized to compute the heat transfer coefficient as well as the convective heat coefficient. The convective heat coefficient is then used to get the convective heat coefficient. According to the literature and to the best knowledge of the authors, an experimental investigation on analysis of effective parameters on the combined heat transfer and pressure drop properties in a corrugated plate heat exchanger with nanofluid has not yet been considered. As a result, the focus of this research is to find the best conditions for increasing heat transfer rate and lowering pressure drop in a corrugated plate heat exchanger, which might serve as a beneficial guideline for heat transfer researchers. The heat transfer parameters and pressure drop of a CPHE (corrugated plate heat exchanger) were explored experimentally using a chemically synthesised ZnO/sparkling water Nanofluid, which is the topic of this article.

1.1. Nanofluid preparation

ZnO manufacture may be divided into two categories: High energy consumption, poor purity, uneven particle size distribution, large volumes of secondary waste and long-term environmental damage are only some of the problems associated with physical processes. Chemical processes, on the other hand, benefit from low energy consumption, high purity, consistent particle size distribution, low cost, and minimum environmental impact. It is becoming more important to synthesise ZnO materials in ecologically benign methods as the number of ZnO uses grows, especially now that the public's expectations for environmental preservation have been instilled according to Anbuvannan et al. [19]. Use of microorganisms, plant extract and plant enzymes in the chemical reaction process is a green synthesis approach. The production of ZnO may be stabilized and reduced by extracts from plants such as peels, flowers, fruits, and seeds, as well as from leaves, peels, roots, and other parts of the plant. ZnO formation may be reduced and stabilized by using these extracts, according to research. It is possible to make zinc oxide using plant extracts, which results in a zinc oxide that is more effective against a wide spectrum of bacteria than chemically synthesized zinc oxide was investigated by Vijayakumar et al. [20]. To use these compounds in products that will come into contact with the human body, they must be non-toxic and mild. Environmentally friendly growth may be facilitated by the use of plant extracts in the production of green zinc oxide in the future .This approach is used to manufacture nanoparticles from extracts of the Hibiscus rosa-sinensis leaf, which is the subject of this research. A leaf extract of roughly 50 mL was obtained and heated at 70°C with a stirrer for 15 min. Due to the high temperature, 5 g of zinc nitrate were added to the solution before it was applied. Cooking happens before the addition of a yellow-colored paste to the mixture. A ceramic crucible was used to collect the paste, which was heated in a furnace at 400°C for 2 h to collect the paste. It produces a powder of a soft white tint that may be collected and utilized for a variety of other uses. Nanofluids are created using chemically generated zinc oxide nanoparticles with diameters ranging from 100 nm to 99% purity, which has been purified to 99% purity. CTAB, a surfactant, is also used to prepare these particles, and it is used to do so. The following is the procedure to be followed to create nanofluids: The solution should be added to dilute water and then treated to an ultrasonic granulator for 30 min to get the optimum results. To get the desired amplitude, the ultrasonic aided Machining vibrator is set to 0.6 on the scale. It is used in the vibration of ZnO nanoparticles. Fig. 1 shows a transmission electron microscope image of nanoparticles of ZnO and a sample of the nanofluid that was generated.

1.2. X-ray diffraction pattern of zinc oxide

A goniometer is an angle measurement equipment that is particularly helpful for measuring the angles between the faces of crystals. Goniometer uses Cu-α radiation in the 2-range of 10–80 nm for the X-ray diffractometer, which is a wavelength between 10 and 80 nm. The Debye–Scherrer formula and the Debye–Scherrer formula are used in X-ray diffraction analysis to compute the starting condition and measurement in a goniometer with a radius of 217.5 mm, a step duration of 30.6 s, and a step size of 30.6 nm (0.0289093). The greatest intensity detected in this analysis is 67.45° out of 1,125 counts, which is the highest attainable. Peak intensity levels and wide diffraction patterns show crystallinity, which suggests that the particles under study have an extremely tiny crystallite size which is shown in Fig. 2.

2. Experiments

2.1. Experimental setup

Heat exchangers are used in a variety of different applications, including refrigeration and heat pump systems. As seen in Fig. 3, these heat exchangers are both more efficient and less costly than equivalent compact heat exchangers of a similar size. The findings of the subsequent trials

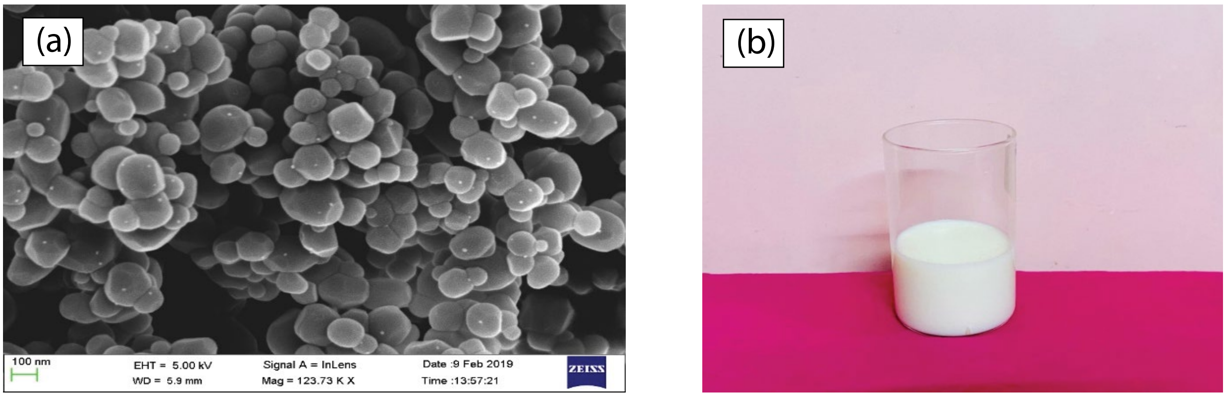

Fig. 1. (a) ZnO nanoparticles as seen using a scanning electron microscopy and (b) nanofluid preparation sample.

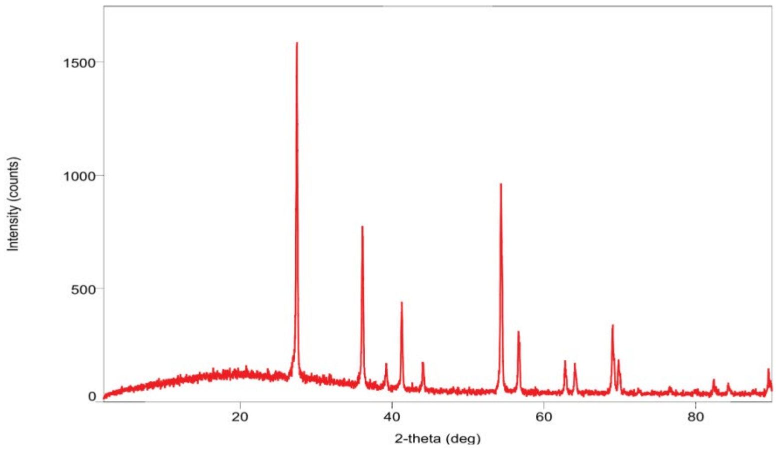

Fig. 2. X-ray diffraction image of TiO_2 nanopowder.

reveal that the system has two distinct flow loops, one for hot fluid and the other for cold fluid. Zinc oxide fluid is a heated liquid solution that has been chemically manufactured. The following components is included in this system: a corrugated plate heat exchanger, two pumps, an electronic thermostat, two reservoir tanks, four type-k thermoelectric couples, two drain containers, and a differential pressure transducer (DPT). Fig. 4 and Table 1 show a schematic of a corrugated heat exchanger and the geometrical characteristics that go along with it. The purpose of any heat exchanger component is to reduce the amount of heat lost by the system. In addition, insulation is employed to prevent heat from escaping from the system. To monitor the temperature and quantity of water going down a drain, rotating metres are utilized. Using four type-k calibrated thermoelectric couples, the intake and output fluid temperatures of a heat exchanger are determined. It is possible to maintain a constant supply of hot water by using a temperature-controlled thermostat and a thermocouple. The difference in pressure between the exchangers is measured with the use of an electronic pressure transducer (EPT). The remaining two 2.5 kW electric heaters supply the remainder of the heating energy for the hot water tank. By keeping the water temperature constant during the experiment, the cold flow rate may be evaluated for accuracy. The varied heat coefficients and Reynolds numbers are calculated based on the work of Kline and McClintock [21].

3. Consolidation of data

3.1. Coefficient of heat transfer

It is as follows, according to the dimensionless form of the Nusselt number of a fluid flowing through a solid surface: Nu = (Re,Pr).

$$\mathrm{Nu} = \nu_1 \mathrm{Re}^{\alpha} \mathrm{Pr}^{\beta} \tag{1}$$

and

$$\mathrm{Nu} = \frac{hD_h}{\lambda_f} \tag{2}$$

where λ_f is indeed the fluid's thermal conductivity and D_h is the channel's hydraulic diameter, which seems computed as follows [22]:

$$D_h = \frac{4 \times \text{Channel Flow Area}}{\text{Wetted Perimeter}} = \frac{4bW}{2(b+w)} = 2b \tag{3}$$

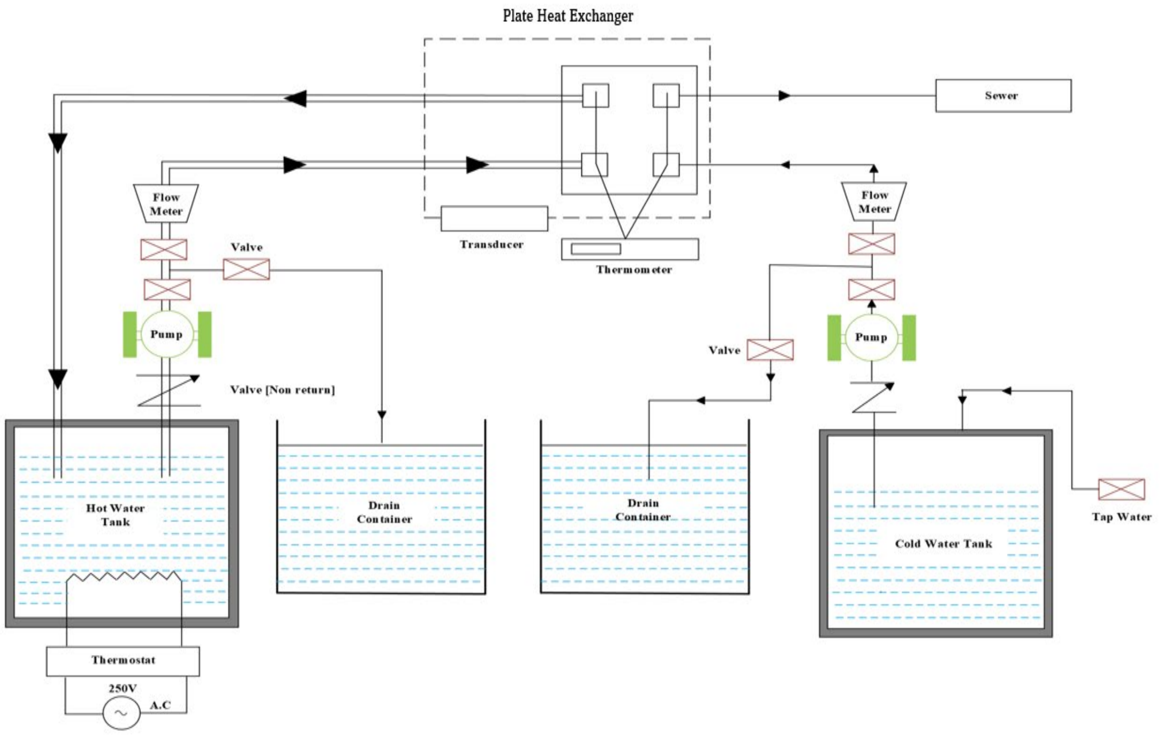

Fig. 3. Diagram of the experimental setup.

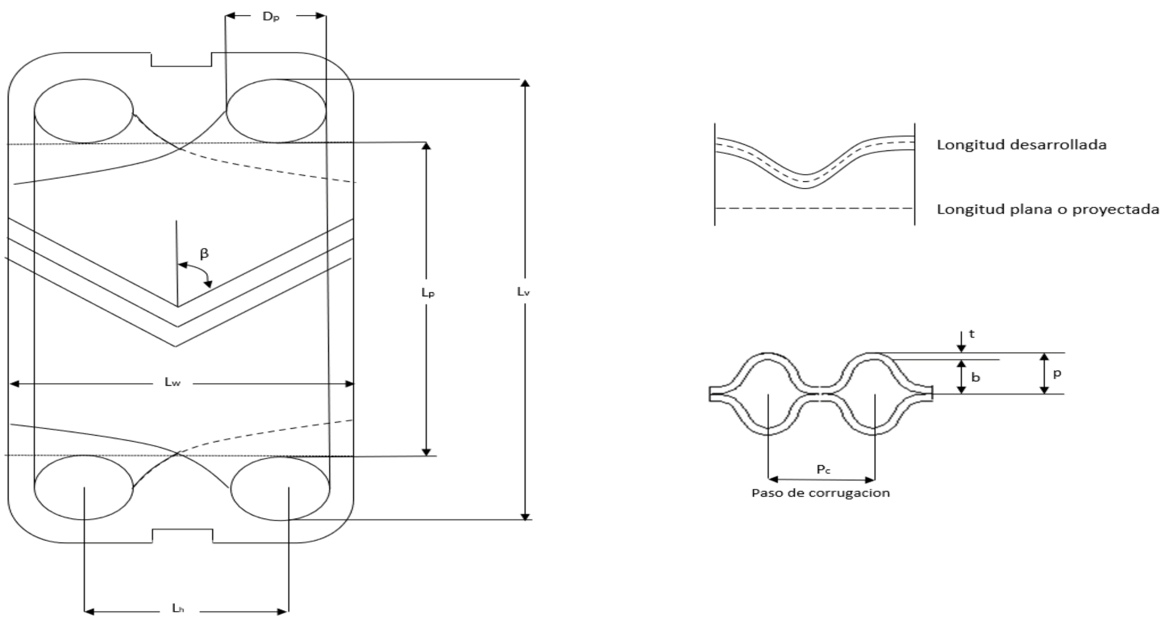

Fig. 4. Diagram of the heat exchanger plate.

where W is the channel width, whereas b denotes the distance between the two plates. b is little when compared to W, so, $W \cong b + W$.

The coefficient of net heat transfer U, which is given in Eq. (2), may be used to calculate the energy transfer coefficient.

$$\frac{1}{U} = \frac{1}{h_h} + \frac{\Delta x}{k_m} + \frac{1}{h_c} \tag{4}$$

where h_h is the film coefficient coefficient by convection of hot liquid and h_c is the film coefficient by convection of

Table 1
Geometrical parameters for CPHE

Specification	Measurements
Heat exchanger length (L), m	0.184
Breadth of the heat exchanger (W), m	0.06
Length from one port to another (L_p), m	0.148
Corrugated plate's number (N)	16
For the hot side, a certain amount of channels are offered (N_h)	7
For the chilly side, there are a certain number of channels (N_c)	8
Angle of the chevron (β)	45°
CPHE thickness in millimetres	0.030
Δx is thickness of the plate	0.0002
Distance in the space between two plates (b), m	0.00221
Pitch of corrugation (Pc), m	0.006

cold liquid, Δx is the width of the heat exchanger's plate, and k_m is the heat conductivity of unstained steel. The convective heat transfer coefficient may be used to assess the effectiveness of heat transmission between hot and cold liquids. This number is derived from the plate's thermal conductivity and the heat exchanger's width. The following formula may be used to get the overall heat efficiency:

$$Q = \dot{m}\text{Cp}_h\left(T_{\text{hi}} - T_{\text{ho}}\right) = UA\Delta T_{\text{LMTD}} \tag{5}$$

A denotes the CPHE heat transfer region and ΔT_{LMTD} is calculated by taking the average temperature difference. Eqs. (6) and (7) provide the following parameters:

$$A = N \times L \times W \tag{6}$$

As N and L are the number of corrugated plates and their length, respectively.

$$\Delta T_{\text{LMTD}} = \frac{\left(T_{\text{hi}} - T_{\text{ci}}\right) - \left(T_{\text{ho}} - T_{\text{co}}\right)}{\text{Ln}\left(\dfrac{T_{\text{hi}} - T_{\text{ci}}}{T_{\text{ho}} - T_{\text{co}}}\right)} \tag{7}$$

On the other hand, the temperature difference between T_{ci} and T_{co} is indicated by the outlet and inlet temperature of a heat exchanger. Because of the CPHE's set material and geometrical factors, the metal wall resistance ($\Delta x/k_m$), it is regarded as constant. Also, the thermal resistance of cold fluid almost always remains constant due to the fixed volume velocity and the temperature variations are minor. Due to the thermal resistance ($1/h_c$), of cold fluid, it is solely determined by the hot fluid coefficient of heat transfer. Furthermore, the thermal efficiency of the hot fluid is the sole way to characterize the whole heat transfer coefficient of the hot fluid. Under some conditions, such as when the average temperature of the fluid fluctuates due to variable flow rate, the fluid's system characteristics may be reformulated with the help of Eqs. (1) and (2) as follows:

$$\frac{1}{U} = \frac{1}{h_h} + c = \frac{m}{u^{\alpha}} + c \tag{8}$$

It is determined by the factors m and c how quickly a heated fluid moves across space. In this experiment, the range of Reynolds numbers used is 179–579, which shows that the experiments are being carried out in a turbulent flow situation [23]. It is also well known that the value of is determined from the intercept of the plot concerning the turbulent flow, as shown in the figure. It has been established that the value is around 2/3 in a turbulent flow. The intercept of $1/U$ vs. $1/u$ shown on the graph may be used to determine h_h. Eqs. (9) and (10) estimate the sensible heat lost by the hot fluid and the sensible heat obtained by the nanofluid based on the mass flow rate, specific heat, and temperature differential (hot and nanofluid) between the hot fluid and the nanofluid may be calculated by using Saleh et al. [24].

$$Q_h = m_h c_{\text{ph}}\left(T_{\text{hi}} - T_{\text{ho}}\right) \tag{9}$$

$$Q_{\text{nf}} = m_{\text{nf}} c_{\text{pnf}}\left(T_{\text{nf},o} - T_{\text{nf},i}\right) \tag{10}$$

3.2. Deflation of pressure

CPHE diffusive pressure, on the other hand, is composed of frictional pressure reductions in tubes and dips in ports as a result of the flow of fluid.

$$\Delta P_t = \Delta P_{\text{ch}} + \Delta P_p \tag{11}$$

The Darcy friction factor model is used to calculate the channel pressure drop:

$$\Delta P_{\text{ch}} = 4f\left(\frac{L_p}{D_h}\rho\frac{u^2}{2}\right) \tag{12}$$

The friction factor of a channel may be calculated using Focke's model [25] and the correlation between the entry and outflow ports. The density of the fluid is represented by the letter L_p, while the distance between the centres of the ports is represented by the term port-to-port length (both input and output). To estimate the pressure loss between the ports, the Focke and the Shah [26] correlation is employed as a tool.

$$\Delta P_p = 1.5\frac{\rho u^2}{2} \tag{13}$$

3.3. Thermophysical properties of nanofluids

It is necessary to determine the thermal conductivity of nanofluid from the outset to establish an agreeable agreement between theoretical and experimental data. The H-C model [27] is used to estimate the thermophysical characteristics of nanofluids. In most fluid thermal conductivity calculations, this model is used.

$$k_{\mathrm{nf}} = \left[\frac{k_p + (m-1)k_t - (m-1)\varnothing(k_t - k_p)}{k_p + (m-1)k_t + \varnothing(k_t - k_p)}\right]k_t \tag{14}$$

These are two characteristics of spherical particles that may be assessed based on their thermal conductivity: the empirical form factor N and the sphericity. It is one when considering the sphericality of a spherical item. The thermal conductivity of nanoparticles and the thermal conductivity of base fluids are denoted by the letters k_{nf} and k_p, respectively. Murshed et al. [28] estimated the thermal conductivity of nanofluids, Bruggeman developed the following model, which can be expressed mathematically as:

$$k_{\mathrm{nf}} = 0.25\left[(3\varnothing - 1)k_p + (2 - 3\varnothing)k_t\right] + \frac{k_t}{4}\sqrt{\Delta} \tag{15}$$

$$\Delta = \left[(3\varnothing - 1)^2\left(\frac{k_p}{k_t}\right)^2 + (2 - 3\varnothing)^2 + 2\left(2 + 9\varnothing - 9\varnothing^2\right)\left(\frac{k_p}{k_t}\right)\right] \tag{16}$$

Yu and Choi [29] suggested the following new mathematical equation for estimating thermal conductivity:

$$k_{\mathrm{nf}} = \left[\frac{k_p + 2k_t - 2\varnothing(k_t - k_p)(1+\beta)^3\varnothing}{k_p + 2k_t + \varnothing(k_t - k_p)(1+\beta)^3\varnothing}\right]k_t \tag{17}$$

where β is the ratio of nano-layer thickness to original particle radius. The thermal efficiency of a nanofluid is calculated using b = 0.1. The notion of the effective medium, introduced by Timofeeva et al. [30], is used to compute thermal conductivity of nanofluids and is stated as follows:

$$k_{\mathrm{nf}} = \left[1 + 3\varnothing\right]k_t \tag{18}$$

It is possible to determine the thermal conductivity of microfluids by using many theoretical methodologies. The viscosity of a nanofluid is a significant component in influencing its performance. This research examines how well-known models predict outcomes and compares them to the actual findings. Batchelor [31] recommends that viscosity be calculated using a straightforward equation for fluids containing sphere-shaped nanoparticles.

$$\mu_{\mathrm{nf}} = \left(1 + 2.5\varnothing + 6.2\varnothing^2\right)\mu_t \tag{19}$$

The Einstein equation for determining the viscosity of spherical particles of volume is proposed by Drew and Passman [32].

$$\mu_{\mathrm{nf}} = (1 + 2.5\varnothing)\mu_t \tag{20}$$

Brinkman [33] reduced Einstein's equation to a simple mathematical structure, which is represented as follows:

$$\mu_{\mathrm{nf}} = \frac{1}{(1-\varnothing)^{2.5}}\mu_t \tag{21}$$

Wang et al. [34] proposed a model for calculating nanofluid viscosity, which can be stated as:

$$\mu_{\mathrm{nf}} = \left(1 + 7.3\varnothing + 123\varnothing^2\right)\mu_t \tag{22}$$

where Ø is the molecule volumetric fixation, μ_{nf} is the consistency of the nanofluid and μ_t is the thickness of the therminol or the base liquid. The relative physical properties of nanofluids and base fluid (x) are flaunted in Fig. 5. In addition, the thermal conductivity of nanoparticles has improved by about 0.018%, 0.009%, and 0.019%, respectively at 0.2%, 0.6% and 1.0% weight percentage of nanoparticles.

4. Discussion of findings

To confirm that the experiments are genuine, the coefficients of convective heat transfer of various working fluids are compared. The calculated convective heat coefficient is compared to that of sparkling water, which is employed as a working fluid. The method used to transmit heat to a water-to-plate heat exchanger has been tried and tested. The convective heat transfer coefficient between sparkling water and the working fluid when the system is in a single-phase condition.

The computed data shows that the performed experiments are valid. As shown in Fig. 6, the Reynolds number and the weight share of the nanoparticles have an impact on convective heat transfers. Data tendency increases at Reynolds number 320 due to the increasing turbulence intensity. It is believed that this increase in turbulence intensity is caused by the reduction of the fluid viscosity within the walls shown in Fig. 7. The heat transfer rate of nanofluids can be optimized by improving the thermal conductance of nanoparticles. This effect is caused by the random movement of nanoparticles in a fluid. In addition, the maximum enhancement of the corporatization heat transfer coefficient depends on the volume and weight engrossment of the nanoparticles. For instance, the flow rate of nanoparticles at 0.3% and 1.5% is higher than the flow rate of nanoparticles at 0.6% and 0.8% which is shown in Fig. 8.

Table 2 summarises some of the research on nanofluid heat transfer performance that has been published. It gives an approximation of the experimental data for convective thermal conductivity in nanofluids.

Fig. 9 depicts the heat transfer coefficient between different weight fractions of nanoparticles. Several researchers have hypothesized that the Reynolds number and weight % of the nanoparticles have an impact on the overall efficiency of heat transfer. At 0.2%, 0.6%, and 1.0% weight percentages of nanoparticles, the thermal efficiency of nanoparticles has been improved by about 2.8%, 5.7%, and 8.9%, respectively.

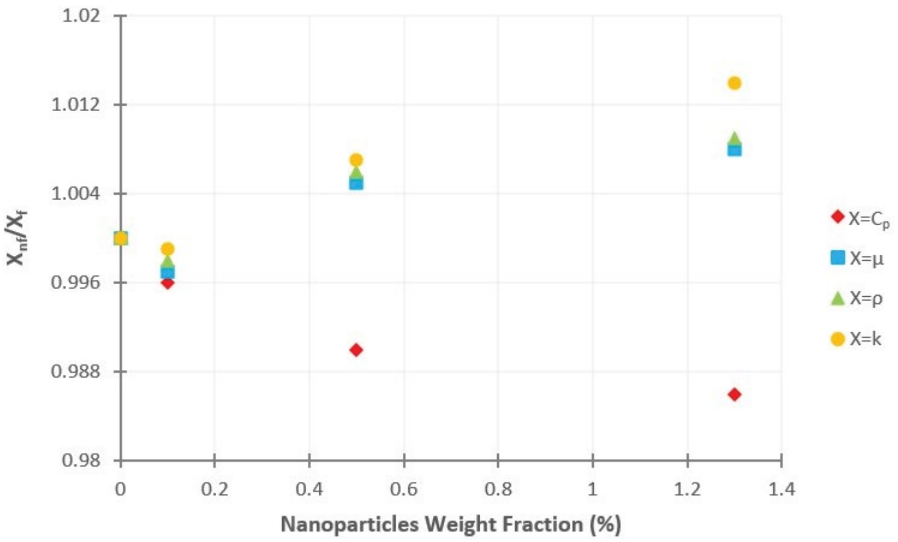

Fig. 5. Changes in relative physical characteristics as an element of nanoparticle weight percentage.

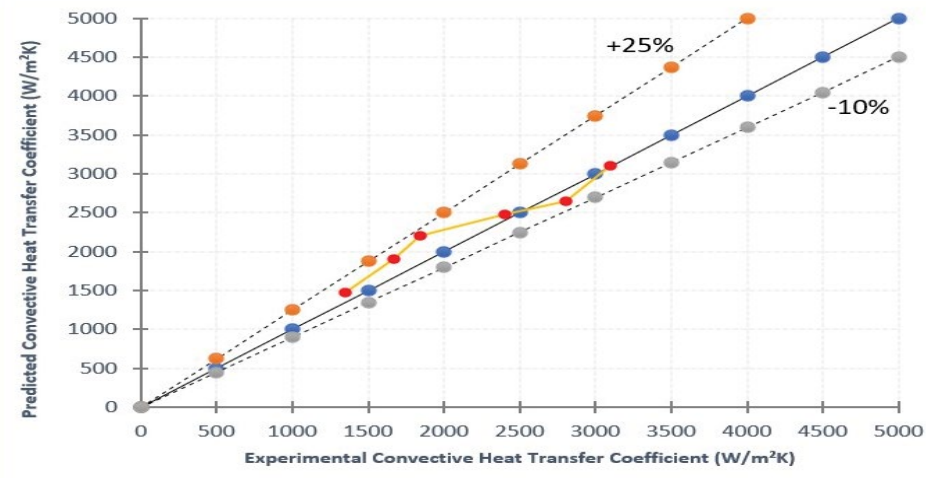

Fig. 6. Comparison of estimated and experimental convective heat transfer coefficients for sparkling water in CPHE.

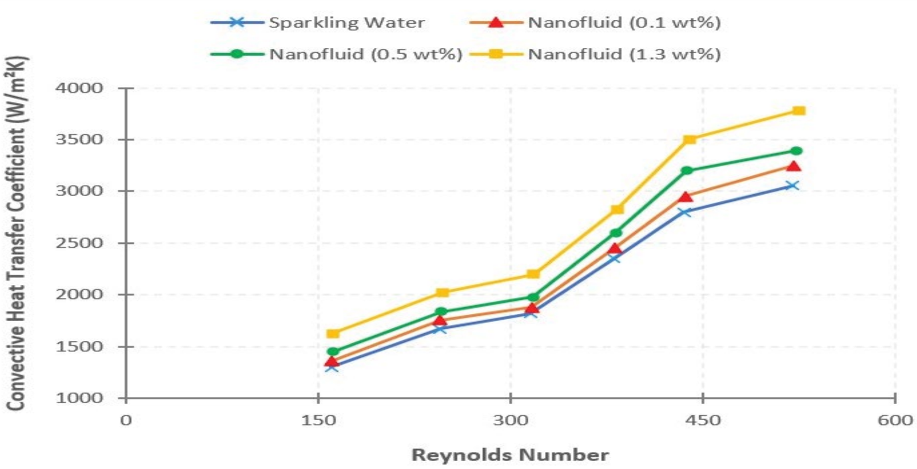

Fig. 7. Comparison of the convective transfer of heat coefficients of TiO_2 nanofluid at different weight fractions and sparkling water in CPHE.

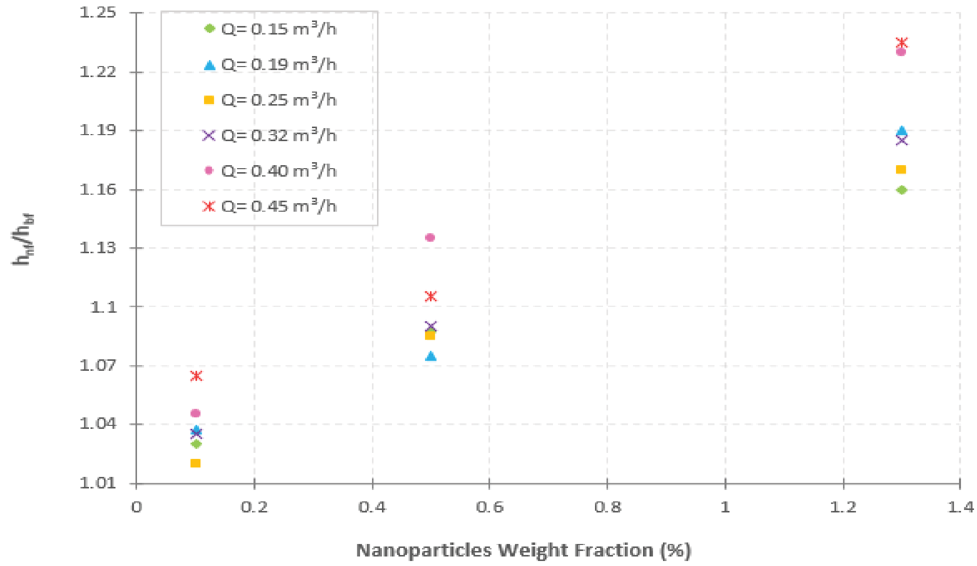

Fig. 8. Fluctuation of the relative convective transfer heat coefficient as a function of nanoparticle weight concentration at various nanofluid flow speeds.

Eq. (9) compares computed pressure drop with calculated pressure drop values. The results show that experimental data differs little from expected data shown in Fig. 10.

Fig. 11 depicts how the pressure differential drop of a given nanofluid increases linearly as the fluid's weight% and Reynolds number rise. The pressure drop that nanofluid can lower by 20% is the utmost feasible. The raise in viscosity and density of the nanofluid may be ascribed to an increase in viscosity and density of the nanofluid when compared to sparkling water. The outcome indicates that the use of nanofluids may help to reduce pressure spikes in the system.

5. Conclusion

In a corrugated plate heat exchanger, the characteristics of heat transfer and pressure drop of a ZnO-sparkling water nanofluid were examined. The investigations are carried out using a heated fluid flowing in a turbulent flow. As a function of Reynolds number and nanoparticle weight concentrations, we investigate the link between pressure drop and heat transmission.

- The results show that adding ZnO nanoparticles to sparkling water improves the solution's heat transfer properties dramatically.
- The findings of this research demonstrate that increasing the Reynolds number and the weight % of nanoparticles increases the efficiency of nanofluid heat transfer.
- The thermal conductivity of nanofluids has been demonstrated to vary from 2.9% to 25.7%, while the convective heat conductivity varies from 12.8% to 9.5%. To enhance the mechanical properties of fluids, a range of characteristics such as heat capacity may be used. This may be accomplished using metal oxide nanoparticles. They may produce frictional force between the particles in the system by varying the thickness of the shear layer.
- Injecting nanofluids into a system has been shown to enhance the pressure drop over a corrugated plate heat exchanger. However, if the technology is not used properly, this growth may be overlooked.
- This study effort demonstrates that nanofluid may be used as a heat transfer fluid in a range of applications, including hot water systems and industrial operations, due to its enhanced qualities.

Author contributions

Conceptualization, W.A.; methodology, investigation and analysis; Z.Z.C., S.N.K. and M.R.B.J.; supervision, project administration and resources, I.A.B. and M.E.M.S.; reviewing and proofreading, M.A.M. and M.G.; analysis of thermophysical properties, formal analyses, review and editing, S.K. and T.M.Y.K. All authors have read and agreed to the published version of the manuscript.

Data availability statement

The authors confirm that the data supporting the findings of this study are available within the article and its Supplementary Materials.

Disclosure statement

"The authors declare that he has no relevant or material financial interests that relate to the research described in this paper".

Symbols

Q	—	Rate of heat transfer, W
U	—	Coefficient of total heat transfer, W/m²K
H	—	Coefficient of convective heat transfer, W/m²K

Table 2
Overview of many experimental studies on the heat transfer capabilities of nanofluids that have been published in peer-reviewe journals

Investigator	Nanofluid	Nanoparticle dimensions	Fraction of volume	Section of testing	Re or flow rate range	HTC or Nu range	Outcome
1. Barzegarian et al. [22]	Water-TiO_2	20 nm	0.3, 0.8 and 1.5 wt.%	Brazed plate heat exchanger	Re ~ 157–529.1 and rate of flow (lpm) ~ 2.4–7.5	Nu ~ 9–24 and HTC ~ 1,400–3,800	HTC is improved by 6.6%–23.7%
2. Huang et al. [14]	Water-Al_2O_3 and water-MWCNT	40 nm (Al_2O_3) and 9.51 nm (MWCNT)	2.19–10.35 wt.% (Al_2O_3) and 0.03–0.1 wt.% (MWCNT)	Chevron plate heat exchanger	Re ~ 59–617	1,050–6,900 ~ HTC (Water-Al_2O_3) and 820–6,550 ~ HTC (Water-MWCNT)	HTC of both nanofluids is lower as compared to the base fluid
3. Pantzali et al. [9]	Water-CuO	30–50 nm	0.015, 0.031, 0.039, 0.78, 0.118, 0.157 and 0.236 vol.%	Circular tube	Re ~ 55,000–31,000	6,300–24,200 ~ HTC	On average, HTC is improved by 25%
4. Sarafraz et al. [36]	Water-MWCNT	–	0.5, 1 and 1.5 vol.%	Plate heat exchanger	Re ~ 140–15,000	Nu ~ 9.6–80	Nu augmentation of 7 and 14% at 0.5 and 1 vol.%
5. Duangthong-suk and Wong-wises [8]	Water-TiO_2	20 nm	0.2 vol.%	Double tube heat exchanger	Re ~ 5,500–17,000	HTC ~ 3,820–9,120	HTC is improved by 6%–11%
6. Tiwari et al. [13]	Water-CeO_2	31 nm	0.5, 0.75, 1, 1.25, 1.5, 2 and 3 vol.%	Plate heat exchanger	Flow rate (lpm) ~ 1–4	HTC ~ 650–1,050	At the optimal nanoparticle volume fraction (0.75 vol.%), the boost is 39%
7. Heris et al. [1]	Water-Al_2O_3	20 nm	0.2, 0.5, 1, 1.5, 2 and 2.5 vol.%	Circular tube	Re ~ 600–2,060	HTC ~ 650–1,150	HTC augmentation of 8%–16% and 22%–41% at 0.2 and 2.5 vol.%, respectively
9. Ahmed et al. [35]	Zinc oxide-ethylene glycol distilled water	30 nm	0.1, 0.075, 0.05 and 0.025 vol.%	Horizontal calibrated circular tube	Re ~ 500–2,160	HTC ~ 550–1,050	HTC augmentation of 8%–18% and 22%–45% at 0.075 and 0.025 vol.%, respectively
7. Present study	Chemically synthesized ZnO-sparkling water	100 nm	0.1%, 0.5%, and 1.3%	Corrugated plate heat exchanger	Re ~ 159–538 and rate of flow (lpm) ~ 2.4–7.6	HTC ~ 2,500–4,600 and Nu ~ 12–29	HTC improvement ranges from 9.9 to 28.9%

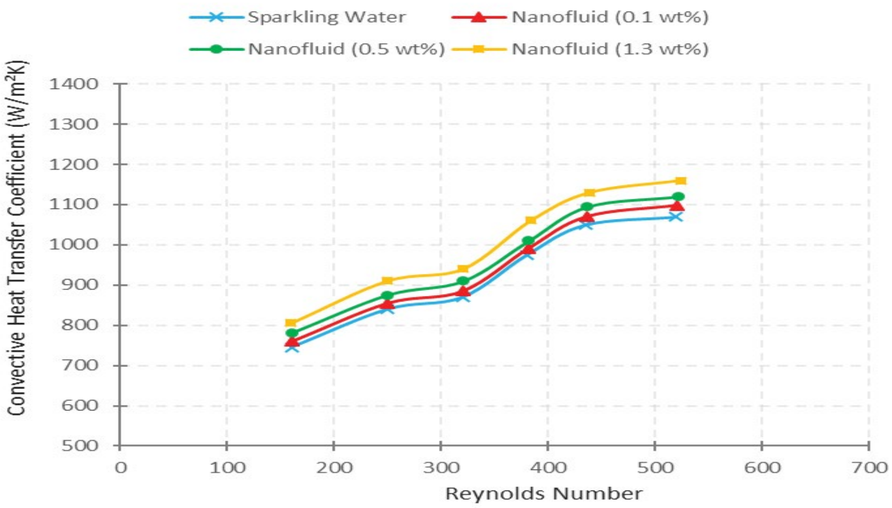

Fig. 9. Comparison of the total heat transfer coefficients of TiO_2 nanofluids at different weight fractions and sparkling water in CPHE.

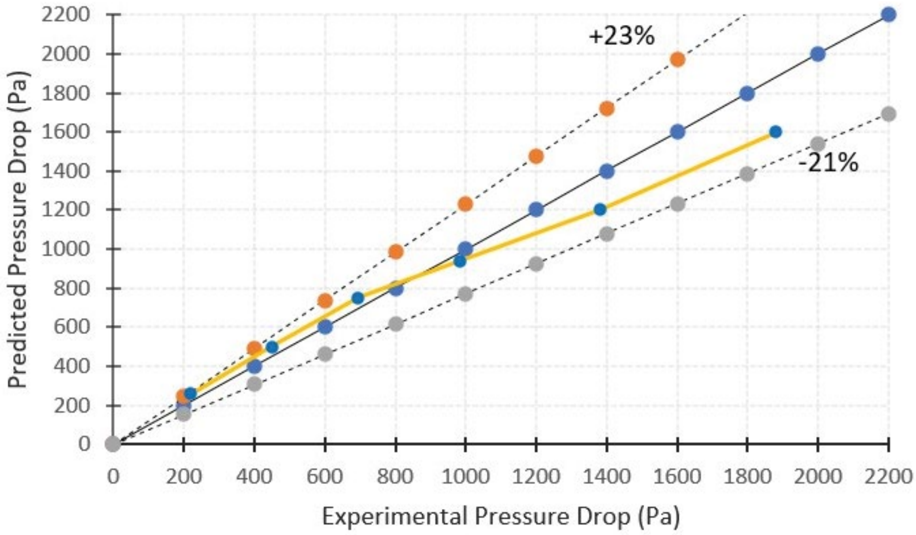

Fig. 10. Comparison of estimated and experimental pressure drops in CPHE for sparkling water.

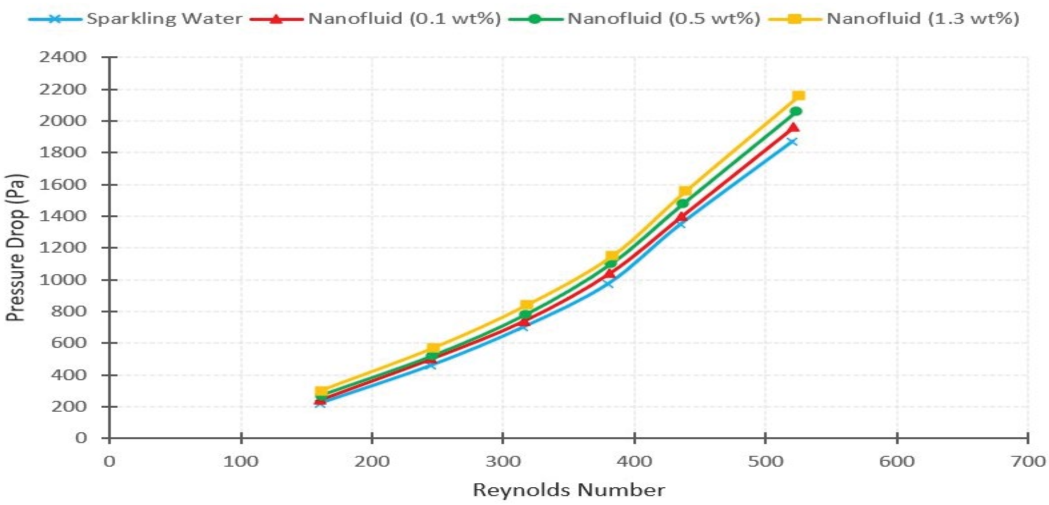

Fig. 11. Pressure decrease of ZnO nanofluid at different weight fractions vs. sparkling water in CPHE.

W	—	Breadth of the channel, m
L	—	Length of the plate, m
N	—	Quantity of corrugated plates
B	—	Chevron angle of CPHE
T	—	Fluid flow's temperature, °C
A	—	Heat exchanger's heat transmission area, m^2
b	—	Distance between two plates, m
M	—	Rate of mass flow, kg/s
U	—	Rate of fluid flow, m/s
C_p	—	Specific heat, J/kg K

Greek

μ	—	Dynamic viscosity, Pa·s
ρ	—	Mass density, kg/m^3
κ	—	Thermal conductivity, W/mK
ϕ	—	Volume concentration

Subscripts

m_o	—	Outer edge
L_p	—	Length from one port to another
m_i	—	Inner edge
D_h	—	Hydraulic diameter of channel, m_c cold fluid
P_c	—	Corrugation pitch, m_h hot fluid
Δx	—	Plate thickness
m_{np}	—	Nanoparticle
ΔT_{LMTD}	—	Logarithmic mean temperature difference
Δp_t	—	Total pressure drop, pa, f fluid
Δp_{ch}	—	Decline in channel pressure, pa
Δp_p	—	Pressure in the ports drops, pa, nf nanofluid
Re	—	Reynolds number, ρUD/μ water
Pr	—	Prandtl number, C_p μ/k
Nu	—	Nusselt number, h D/k

Abbreviations

f	—	Friction factor
HTC	—	Film coefficient
CPHE	—	Corrugated plate heat exchanger

References

[1] S. Zeinali Heris, S.Gh. Etemad, M. Nasr Esfahany, Experimental investigation of oxide nanofluids laminar flow convective heat transfer, Int. Commun. Heat Mass Transfer, 33 (2006) 529–535.

[2] K.B. Anoop, T. Sundararajan, S.K. Das, Effect of particle size on the convective heat transfer in nanofluid in the developing region, Int. Commun. Heat Mass Transfer, 52 (2009) 2189–2195.

[3] U.K. Ahmad, M. Hasreen, N.A. Yahaya, B. Rosnadiah, Comparative study of heat transfer and friction factor characteristics of nanofluids in rectangular channel, Procedia Eng., 170 (2017) 541–546.

[4] L. Xu, J.L. Xu, Nanofluid stabilizes and enhances convective boiling heat transfer in a single microchannel, Int. Commun. Heat Mass Transfer, 55 (2012) 5673–5686.

[5] Z. Edalati, S.Z. Heris, S.H. Noi, The study of laminar convective heat transfer of CuO/water nanofluid through an equilateral triangular duct at constant wall heat flux, Heat Transfer – Asian Res., 41 (2012) 418–429.

[6] M. Hojjat, S.Gh. Etemad, R. Bagheri, J. Thibault, Laminar convective heat transfer of non–Newtonian nanofluids with constant wall temperature, Heat Mass Transfer, 47 (2011) 203–209.

[7] Y. Yang, Z.G. Zhang, E.A. Grulke, W.B. Anderson, G. Wu, Heat transfer properties of nanoparticle in-fluid dispersions (nanofluids) in laminar flow, Int. J. Heat Mass Transfer, 48 (2005) 1107–1116.

[8] W. Duangthongsuk, S. Wongwises, Heat transfer enhancement and pressure drop characteristics of TiO_2–water nanofluid in a double-tube counter flow heat exchanger, Int. J. Heat Mass Transfer, 52 (2009) 2059–2067.

[9] M.N. Pantzali, A.G. Kanaris, K.D. Antoniadis, A.A. Mouza, S.V. Paras, Effect of nanofluids on the performance of a miniature plate heat exchanger with modulated surface, Int. J. Heat Fluid Flow, 30 (2009) 691–699.

[10] C.S. Jwo, L.Y. Jeng, T.P. Teng, C.C. Chen, Performance of overall heat transfer in multi-channel heat exchanger by alumina nanofluid, J. Alloys Compd., 504S (2010) S385–S388.

[11] M. Chandrasekar, S. Suresh, A. Chandra Bose, experimental studies on heat transfer and friction factor characteristics of Al_2O_3-water nanofluid in a circular pipe under laminar flow with wire coil inserts, Exp. Therm. Fluid Sci., 34 (2010) 122–130.

[12] M.K. Moraveji, S. Razvarz, Experimental investigation of aluminum oxide nanofluid on heat pipe thermal performance, Int. Commun. Heat Mass Transfer, 39 (2012) 1444–1448.

[13] A.K. Tiwari, P. Ghosh, J. Sarkar, Heat transfer and pressure drop characteristics of CeO_2/water nanofluid in plate heat exchanger, Appl. Therm. Eng., 57 (2013) 24–32.

[14] D. Huang, Z. Wu, B. Sundén, Pressure drop and convective heat transfer of Al_2O_3/water and MWCNT/water nanofluids in a chevron plate heat exchanger, Int. J. Heat Mass Transfer, 89 (2015) 620–626.

[15] P.V. Durga Prasad, A.V.S.S.K.S. Gupta, M. Sreeramulu, L. Syam Sundar, M.K. Singh, A.C.M. Sousa, Experimental study of heat transfer and friction factor of Al_2O_3 nanofluid in U-tube heat exchanger with helical tape inserts, Exp. Therm. Fluid Sci., 62 (2015) 141–150.

[16] D.R. Ray, D.K. Das, R.S. Vajjha, Experimental and numerical investigations ofnanofluids performance in a compact minichannel plate heat exchanger, Int. J. Heat Mass Transfer, 71 (2014) 732–746.

[17] M.C.S. Reddy, V.V. Rao, Experimental investigation of heat transfer coefficient and friction factor of ethylene glycol water based TiO_2 nanofluid in double pipe heat exchanger with and without helical coil inserts, Int. Commun. Heat Mass Transfer, 50 (2014) 68–76.

[18] B.X. Wang, X.F. Peng, Experimental investigation on liquid forced-convection heat transfer through microchannels, Int. J. Heat Mass Transfer, 37 (1994) 73–82.

[19] M. Anbuvannan, M. Ramesh, G. Viruthagiri, N. Shanmugam, N. Kannadasan, *Anisochilus carnosus* leaf extract mediated synthesis of zinc oxide nanoparticles for antibacterial and photocatalytic activities, Mater. Sci. Semicond. Process., 39 (2015) 621–628.

[20] S. Vijayakumar, S. Mahadevan, P. Arulmozhi, S. Subramanian, P.K. Praseetha, Green synthesis of zinc oxide nanoparticles using *Atalantia monophylla* leaf extracts: characterization and antimicrobial analysis, Mater. Sci. Semicond. Process., 82 (2018) 39–45.

[21] S.J. Kline, F.A. McClintock, Describing uncertainties in single-sample experiments, Mech. Eng., 75 (1953) 3–8.

[22] R. Barzegarian, M.K. Moraveji, A. Aloueyan, Experimental investigation on heat transfer characteristics and pressure drop of BPHE (brazed plate heat exchanger) using TiO_2–water nanofluid, Exp. Fluid Therm. Sci., 74 (2016) 11–18.

[23] W.W. Focke, J. Zacahriades, I. Oliver, The effect of the corrugation inclination angle on the thermo hydraulic performance of plate heat exchangers, Int. J. Heat Mass Transfer, 28 (1985) 1469–1479.

[24] B. Saleh, L. Syam Sundar, Experimental study on heat transfer, friction factor, entropy and exergy efficiency analyses of a corrugated plate heat exchanger using Ni/water nanofluids, Int. J. Therm. Sci., 165 (2021) 106935, doi: 10.1016/j.ijthermalsci.2021.106935.

[25] W.W. Focke, J. Zacahriades, I. Oliver, The effect of the corrugation inclination angle on the thermohydraulic performance of plate heat exchangers, Int. J. Heat Mass Transfer, 28 (1985) 1469–1479.
[26] R.K. Shah, W.W. Fock, E.C. Subbarao, R.A. Mashelkar, Plate Heat Exchangers and Their Design Theory, in: Heat Transfer Design, Hemisphere Publishing, Washington D.C., 1988.
[27] R.L. Hamilton, O.K. Crosser, Thermal conductivity of heterogeneous two component systems, Ind. Eng. Chem. Fundam., 1 (1962) 187–191.
[28] S.M.S. Murshed, K.C. Leong, C. Yang, Enhanced thermal conductivity of TiO_2-water based nanofluids, Int. J. Therm. Sci., 44 (2005) 367–375.
[29] W. Yu, S.U.S. Choi, The role of interfacial layers in the enhanced thermal conductivity of nanofluids: a renovated Maxwell model, J. Nanopart. Res., 5 (2003) 167–171.
[30] E.V. Timofeeva, A.N. Gavrilov, J.M. McCloskey, Y.V. Tolmachev, S. Sprunt, L.M. Lopatina, J.V. Selinger, Thermal conductivity and particle agglomeration in alumina nanofluids: experiment and theory, Phys. Rev., 76 (2007) 061203, doi: 10.1103/PhysRevE.76.061203.
[31] G.K. Batchelor, The effect of Brownian motion on the bulk stress in a suspension of spherical particles, J. Fluid Mech., 83 (1977) 97–117.
[32] D.A. Drew, S.L. Passman, Theory of multi component fluids, Appl. Math. Sci., (1999) 105–121.
[33] H.C. Brinkman, The viscosity of concentrated suspensions and solution, J. Chem. Phys., 20 (1952) 571–581.
[34] X. Wang, X. Xu, S.U.S. Choi, Thermal conductivity of nanoparticles–fluid mixture, J. Thermophys. Heat Transfer, 13 (1999) 474–480.
[35] W. Ahmed, Z.Z. Chowdhury, S.N. Kazi, M.R. Bin Johan, I.A. Badruddin, M.E.M. Soudagar, S. Kamangar, M.A. Mujtaba, M. Gul, T.M. Yunus Khan, Evaluation on enhanced heat transfer using sonochemically synthesized stable ZnO-Eg@Dw nanofluids in horizontal calibrated circular flow passage, Energies, 14 (2021) 2400, doi: 10.3390/en14092400.
[36] Z. Li, M. Sarafraz, A. Mazinani, T. Hayat, H. Alsulami, M. Goodarzi, Pool boiling heat transfer to CuO-H_2O nanofluid on finned surfaces, Int. J. Heat Mass Transfer, 156 (2020) 119780, doi: 10.1016/j.ijheatmasstransfer.2020.119780.